Two-State Models for Olefin Polymerization using Metallocene Catalysts. 1. Application to Fluxional Metallocene Catalyst Systems

Márcio Nele[†] and Scott Collins*[,‡]

Department of Chemistry, University of Waterloo, 200 University Avenue W., Waterloo, Ontario, Canada N2L 3G1

M. L. Dias[§] and J. C. Pinto*[,||]

Instituto de Macromoléculas Eloísa Mano /IMA and Programa de Engenharia Química/COPPE, Universidade Federal do Rio de Janeiro, Cidade Universitária, CP: 68502, Rio de Janeiro 21945−970 RJ, Brazil

Shirley Lin and Robert M. Waymouth

Department of Chemistry, Stanford University, Stanford, California 94305

Received March 6, 2000; Revised Manuscript Received August 1, 2000

ABSTRACT: A kinetic model was developed to describe the propylene polymerization behavior of fluxional, two-state metallocene catalysts. In particular, the pentad and molecular weight distributions can be described as well as other parameters of interest, such as the weight fraction of crystallizable sequences and the isotactic sequence length distribution, in terms of fundamental kinetic constants and polymerization conditions that pertain to these two-state catalyst systems. The model was used in an attempt to describe the polymerization behavior of two, prototypical, fluxional catalyst systems, $(2\text{-PhInd})_2ZrCl_2$/MAO (**1**) and $(2\text{-}p\text{-}CF_3PhInd)_2ZrCl_2$/MAO (**2**). The model can accurately reproduce the pentad distributions observed in PP prepared using these catalysts and the response of the distribution to changes in polymerization conditions, specifically changes in $[C_3H_6]$ at constant *T*. These studies illustrate that the rate of state-to-state interconversion is slower but of comparable magnitude to the rate of monomer insertion and that the states have similar stability and reactivity. The broad molecular weight distributions previously observed with this family of catalysts can be described by the model. However, the model predicts that the state-to-state interconversion rate has to be significantly slower than the rate of formation of dead polymer chains, and this is inconsistent with the rate estimated from the response of the pentad distribution to changes in the rate of propagation (i.e., $[C_3H_6]$). Recent work where propylene polymerizations using **1** were carried out to low conversion indicate that the broad MWD seen in earlier studies is partly related to variations in $[C_3H_6]$ during polymerization.

Introduction

Fluxional (or conformationally dynamic) metallocene catalysts are an interesting class of polymerization catalysts that can exist in two (or more) conformations (states) during polymer chain formation.[1] In propylene polymerization, these systems can generate a range of different polymer microstructures containing blocks of different stereo-sequences.[1a,b] Stereo-block PP can exhibit elastomeric properties,[2] which have been interpreted as arising from a stereo-block, isotactic-atactic, microstructure generated by two, interconverting isospecific and aspecific states during polymer chain formation (e.g., Scheme 1).[1f,3]

Coleman and Fox first proposed the idea of multistate catalysts in the context of stereo-block polymers formed during anionic polymerization of acrylate monomers.[4] This concept was re-invoked to account for the polymerization behavior of stereorigid, C_1-symmetric,[5] as well as unbridged, 2-arylindene metallocene catalysts.[1f]

Scheme 1

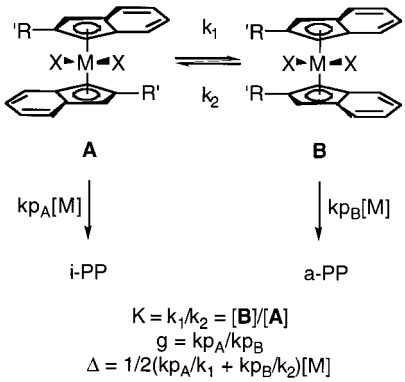

A variety of statistical models were employed in an attempt to estimate the isotactic and atactic sequence lengths from the NMR spectra (i.e., pentad distribution) of the polymers.[5,6] Statistical models of the type employed are most useful when the conditional probabilities, used to describe the microstructure of the polymer, reflect kinetically relevant reaction parameters.

Kinetic (or deterministic) models explicitly account for all relevant elementary steps in the catalytic cycle and represent an alternative approach. Because of their mathematical complexity, kinetic models are less fre-

[†] Current address: Programa de Engenharia Química/COPPE, Universidade Federal do Rio de Janeiro, Rio de Janeiro, Brazil.
[‡] Current address: Department of Polymer Science, University of Akron, Akron, OH 44325-3909.
[§] Instituto de Macromoléculas Eloísa Mano /IMA, Universidade Federal do Rio de Janeiro.
[||] Programa de Engenharia Química/COPPE, Universidade Federal do Rio de Janeiro.

10.1021/ma000401z CCC: $19.00
Published on Web 09/08/2000

quently employed for description of polymer microstructure;[7] nevertheless, such models provide powerful and predictive hypotheses about how the reaction variables are likely to influence the behavior of catalysts and the structure and properties of the resultant polymers.

This latter approach has been used to describe the polymerization behavior of 2-arylindenylmetallocene catalysts under a specific set of conditions: in particular, the variation in block lengths produced by each state as a function of the rate of isomerization between states with identical stability/reactivity was explored.[8] However, a kinetic model has not been generalized for use in modeling, e.g., pentad or molecular weight distributions or for extracting fundamental parameters of interest from these distributions.

In this paper, we develop a kinetic model for fluxional catalysts, which should be generally applicable to these systems.[1] Here, the model is illustrated with reference to the polymerization behavior of unbridged, 2-arylindene metallocene catalysts, and the influence of the isomerization process on the polymer stereo-sequence and molecular weight distributions as well as predictions of polymer crystallinity is investigated.

Results and Discussion: Conceptual Development

It is worth reviewing some general features thought to be pertinent to fluxional catalysts, specifically 2-arylindene metallocene catalysts, and their behavior in propylene polymerization in developing the kinetic model and its application to these systems.

As shown in Scheme 1, these catalysts can exist in two states that may interconvert during polymerization by the process of indenyl ring rotation (with rate constants k_1 and k_2). One of these states is assumed to be isospecific (**A**) and produces isotactic PP (i-PP) at a rate $= k_{p_A}[A][M]$ where [M] is monomer concentration,[9] whereas the other is aspecific (**B**) and produces atactic PP (a-PP) at a different rate $= k_{p_B}[B][M]$. If interconversion between states is slow compared to the rate of propagation (from each state), a block copolymer of a-PP and i-PP should result that may exhibit elastomeric properties (vide infra).

Moreover, as suggested by the mechanism depicted in Scheme 1, the block lengths produced by each state, and as a result the polymer microstructure, should be sensitive to changes in the rate of propagation with respect to state-to-state interconversion.

We have defined a variable (Δ) that relates these two rates through eq 1:

$$\Delta = \frac{(k_{p_A}[A] + k_{p_B}[B])[M]}{k_1[A] + k_2[B]} = \frac{(k_{p_A}\Psi + k_{p_B}(1-\Psi))[M]}{k_1\Psi + k_2(1-\Psi)} \quad (1)$$

Ψ is the mole fraction of catalyst in state **A** and is related to the rate constants for isomerization (Scheme 1) by $\Psi = k_2/(k_1 + k_2)$. Substitution of the latter expression for Ψ [and $k_1/(k_1 + k_2)$ for $1 - \Psi$] into eq 1 leads to eq 2.

$$\Delta = \left(\frac{k_{p_A}}{k_1} + \frac{k_{p_B}}{k_2}\right)\frac{[M]}{2} \quad (2)$$

The variable Δ is an average of the propagation rates, weighted by the lifetimes of each state ($=1/k_i$, $i = 1, 2$). As Δ is directly proportional to [M], this variable will be a function of the experimental conditions for polymerization, as well as being distinct for different catalysts under a particular set of conditions.

The polymer microstructure for a given catalyst system at constant [M] should additionally be influenced by the relative amounts of each state during polymerization (governed by $K = [B]/[A]$, Scheme 1) as well as their intrinsic, relative reactivity toward insertion of monomer (governed by the ratio $k_{p_A}/k_{p_B} = g$, Scheme 1). Strictly speaking, the microstructure will be affected by the ratio of the *rates* of insertion from each state given by $k_{p_A}[A]/k_{p_B}[B] = g/K$. This second parameter (g/K) is thus considered to be an intrinsic property for a given catalyst system and is of obvious fundamental interest when comparing different catalysts (at the same values of Δ).

Note that Δ and g/K are related to one another through eq 3, and thus, the variable Δ is a composite of two fundamental parameters, g/K and the ratio of the rate of propagation to isomerization for *one* of the states. For modeling purposes then, it is only necessary to use g/K and this ratio (e.g., k_{p_B}/k_2) as parameters—Δ may then be calculated using eq 3 at any particular value of [M]. In what follows, we have used Δ as a variable when discussing the response of pentad and molecular weight distributions to changes in [M] or other parameters, but this relationship (eq 3) should be borne in mind.

$$\Delta = \left(\frac{g}{K} + 1\right)\frac{k_{p_B}[M]}{2k_2} \quad (3)$$

Finally, the isospecific state is not expected to produce perfectly i-PP (nor a-PP in the case of the aspecific state); the polymer microstructure will also be determined by the intrinsic stereoselectivity of insertion from each state, which we denote as α and β, for states **A** and **B**, respectively, and the model for stereo-control at each state (e.g., enantiomorphic site vs chain-end control[10]).

Thus, four parameters (Δ, g/K, α, and β) are necessary to describe the pentad distribution of PP produced using a particular, fluxional catalyst and only one of these will respond to changes in experimental conditions at constant T (i.e., Δ).

Another feature of two-state, fluxional catalysts relates to the molecular weight distribution (MWD) of the polymer formed.[11] Intuitively, if the states differ significantly in their k_p/k_{tr} characteristics (i.e., in the kinetic chain lengths associated with each state) and the rate of interconversion between them is slow enough compared to the rate of polymerization, one expects, in the limit, an in-reactor blend of e.g. i-PP and a-PP which may possess a broad or even bimodal MWD. Note that one can also expect variations in the MWD (both its breadth as well as the average values) as a function of [M], depending on the mechanisms for chain transfer from both states.

It remains to develop a quantitative model which can account for all of this behavior (much of which has been experimentally observed) and from this perspective, a kinetic model, which can be applied to the description of both pentad and MW distributions and their response to changes in experimental conditions (i.e., specifically changes in monomer concentration at constant T), is most appropriate as it is directly related to the mechanism of polymerization.

Table 1. Propagation and Chain Transfer Steps for a Fluxional Catalyst[a]

propagation	$P_n^A + M \xrightarrow{k_{pA}} P_{n+1}^A$	(10)
	$P_n^B + M \xrightarrow{k_{pB}} P_{n+1}^B$	(11)
chain transfer	$P_n^A + M \xrightarrow{k_{tmA}} Q_n + P_1^A$	(12)
	$P_n^A (+ M) \xrightarrow{k_{thA}} Q_n + P_1^A$	(13)
	$P_n^B + M \xrightarrow{k_{tmB}} Q_n + P_1^B$	(14)
	$P_n^B (+ M) \xrightarrow{k_{thB}} Q_n + P_1^B$	(15)
isomerization	$P_n^A \xrightarrow{k_1} P_n^B$	(16)
	$P_n^B \xrightarrow{k_2} P_n^A$	(17)

[a] P_n^j is a living polymer chain of length n in state j; Q_n is a dead polymer chain of length n; k_{pj} is the kinetic constant for propagation reaction in state j; k_{thj} is the kinetic constant for β-hydrogen elimination in state j; k_{tmj} is the kinetic constant for chain transfer to monomer in state j.

Mechanism for Chain Growth and Stereo-sequence Formation. For the kinetic model, we assume here that each state produces polymer by a mechanism that would lead to first-order kinetics with respect to [M]. In addition, the kinetic model developed assumes that steady-state conditions apply to all actively growing chains, that initiation is instantaneous and the influence of catalyst decay is negligible on the polymer MWD and microstructure. Additionally, in connection with stereo-sequence formation, we assume that the rates of the isomerization process involving the two states, and the intrinsic nature of the states themselves (i.e., the parameters g/K, α, and β) do not depend on the nature of the polymer chain bonded to the metal.

With these assumptions in mind, the kinetic equations that describe chain growth and chain transfer are summarized in Table 1 while those that describe the rates of dyad (i.e., *meso* or *rac* stereo-sequences) formation are depicted in Table 2. In Tables 1 and 2, the superscript associated with each species denotes the state involved while the rate constants and species definitions are given below each table.

In Table 1, we consider chain transfer to monomer (with rate constant k_{tmi}, i = A, B) and β-hydrogen elimination (with rate constant k_{thi}) as the two processes limiting chain growth, while the last two equations account for state-to-state isomerization during chain growth.

In the top portion of Table 2, each step involves enchainment of a particular enantioface of monomer (*R* or *S* for re or si, respectively) at a particular species. For example, the first equation in Table 2 gives the rate of formation of a (new) *R*,*R*-dyad from a species already bearing an *R*,*R*-dyad; note that the newly formed dyad (i.e., *RR*) shares an *R*-configured monomer unit with the dyad associated with the growing chain (Zr^i_{RR}).

With reference to Table 2, the parameters α and β may be defined in terms of the individual rate constants, assuming enantiomorphic site control at each state, by $\alpha = k_{Ar}/(k_{Ar} + k_{As})$ and $\beta = k_{Br}/(k_{Br} + k_{Bs})$, respectively. Chain end control at, e.g., the aspecfic (**B**) state can be invoked without difficulty if desired.

Model Application to Pentad Distributions. The approach summarized in Table 2 can be extended to kinetic formation of *n*-ads, although the number of simultaneous, differential equations to be solved increases as 2^{n+1} where *n* is the number of consecutive steps involved in forming a *n*-ad! As described in the Supporting Information, the system of linear equations that result from these differential equations under steady-state conditions can be solved using standard, matrix decomposition methods,[12] and thus the relative populations of various stereo-sequences of any *n*-ad can be estimated for particular values of the fundamental parameters discussed above. Here we focus on the response of the pentad distribution to changes in these parameters.

Table 2. Formation of Dyad Stereosequences for a Fluxional Catalyst[a]

propagation from state i (i = A, B)	$Zr^i_{RR} + R \xrightarrow{k_{ir}} Zr^i_{RR} + RR$	(18)
	$Zr^i_{RR} + S \xrightarrow{k_{is}} Zr^i_{SR} + RR$	(19)
	$Zr^i_{RS} + R \xrightarrow{k_{ir}} Zr^i_{RR} + RS$	(20)
	$Zr^i_{RS} + S \xrightarrow{k_{is}} Zr^i_{SR} + RS$	(21)
	$Zr^i_{SR} + R \xrightarrow{k_{ir}} Zr^i_{RS} + SR$	(22)
	$Zr^i_{SR} + S \xrightarrow{k_{is}} Zr^i_{SS} + SR$	(23)
	$Zr^i_{SS} + R \xrightarrow{k_{ir}} Zr^i_{RS} + SS$	(24)
	$Zr^i_{SS} + S \xrightarrow{k_{is}} Zr^i_{SS} + SS$	(25)
isomerization	$Zr^A_{RR} \underset{k_2}{\overset{k_1}{\rightleftharpoons}} Zr^B_{RR}$	(26)
	$Zr^A_{RS} \underset{k_2}{\overset{k_1}{\rightleftharpoons}} Zr^B_{RS}$	(27)
	$Zr^A_{SR} \underset{k_2}{\overset{k_1}{\rightleftharpoons}} Zr^B_{SR}$	(28)
	$Zr^A_{SS} \underset{k_2}{\overset{k_1}{\rightleftharpoons}} Zr^B_{SS}$	(29)

[a] Zr^i_{RR} is a polymer chain bearing, e.g., an R,R-dyad in the state i (i = A, B). R or S denote incorporation of monomer by its re or si enantioface, respectively. RR denotes formation of a (new) RR-dyad. k_{ir} denotes the rate constant for insertion of monomer by its *re* enantioface involving state i (i = A, B).

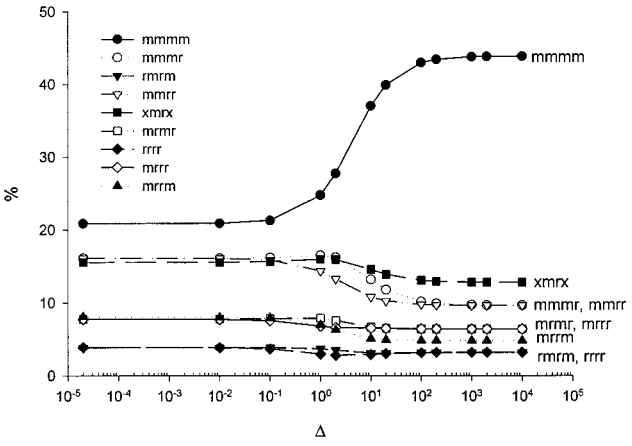

Figure 1. Effect of increasing Δ upon the pentad distribution ($\alpha = 0.96$, $\beta = 0.5$, $g/K = 1.0$).

In Figure 1 is shown the calculated response of the pentad populations to variations in Δ (i.e., [M]) for a particular situation corresponding to $g/K = 1$ with one state isospecific ($\alpha = 0.96$) and the other aspecific ($\beta = 0.5$) assuming enantiomorphic site control for each state.

As with unsymmetrical, *ansa*-metallocene catalysts,[13] two regions corresponding to invariance of the pentad

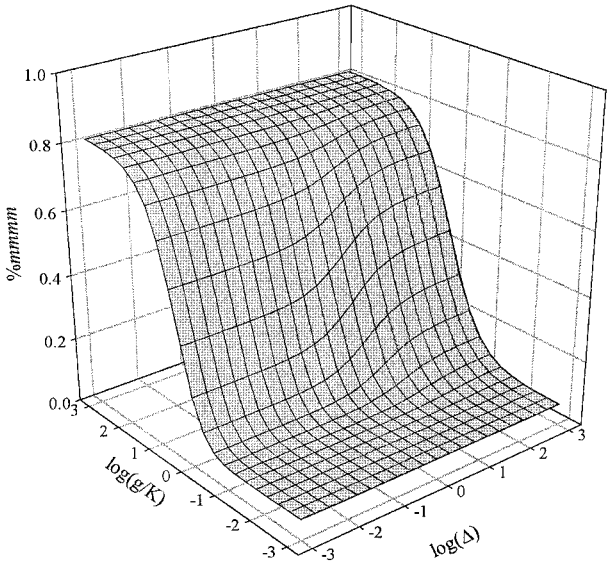

Figure 2. Effect of g/K and Δ upon the population of the mmmm pentad ($\alpha = 0.96$, $\beta = 0.5$).

distribution with Δ (i.e., [M]) can be identified and they correspond to Curtin−Hammett (C−H: $\Delta \ll 1$) and kinetic quenching (KQ: $\Delta \gg 1$) conditions, respectively.

In the Curtin−Hammett regime, the isomerization process is rapid compared to the rate of stereo-sequence formation. In the limit, if isomerization is more rapid than (each) insertion of monomer, the two-state catalyst behaves *identically* to a single-state catalyst and the overall pentad distribution conforms to Bernoullian statistics, governed by a single parameter (in the case of site control) given by[13]

$$\epsilon = \frac{\alpha(g/K) + \beta}{1 + (g/K)} \tag{4}$$

In this regime, the physical significance of g/K is clear. If $g/K \gg 1$ the fluxional catalyst would produce i-PP (ideally isotactic if $\alpha = 1.0$) whereas a-PP (purely atactic if $\beta = 0.5$) would be produced for the converse situation.

To illustrate this point further, Figure 2 shows the response of the mmmm pentad intensity (in %) to changes in Δ for various values of g/K in the form of a surface. It is clear from this figure that significant changes in mmmm (i.e., the pentad distribution) with Δ are only expected if $10^{-1} < g/K < 10^{1}$, otherwise the polymer microstructure is dominated by the more reactive/stable state and is essentially invariant to changes in Δ (i.e., [M]).

Under KQ conditions, the isomerization process is very slow compared to the rate of stereo-sequence formation and a true, blocklike microstructure should result. Note that in this regime, while the pentad distribution may be invariant to further changes in Δ (i.e., [M]) other properties of interest may not (vide infra). In the limit, where the isomerization process is significantly slower than the rate of (dead) polymer chain formation, one ends up with a physical mixture of i-PP and a-PP, the relative amounts of which depend on g/K, and the fluxional catalyst simply behaves as a mixture of two (different), single-state catalysts.

It is important to understand that Δ must change by greater than 3 orders of magnitude to go from one kinetic extreme to the other (see Figure 1) with any particular catalyst. Since monomer concentration can only be practically varied by an order of magnitude at constant T (e.g., from 1 to 10 M at 20 °C), it is possible for fluxional catalysts to show no dependence of the microstructure on [M]. Thus, while a specific dependence of the microstructure to changes in [M] can be a signature of a fluxional catalyst, the absence of such a dependence does not preclude a multistate mechanism.

Under C−H conditions (or where g/K differs greatly from 1), a fluxional catalyst *cannot* be distinguished from a single-state catalyst based on an analysis of, e.g., pentad distributions (or other polymer properties) as indicated above. However, under KQ conditions, a fluxional catalyst may be distinguished from a single-state catalyst (provided $0.1 < g/K < 10$), as the pentad distribution will not conform to Bernoullian statistics even though it may be invariant to changes in [M].

Table 3. Formation of Isotactic Sequences for a Fluxional Catalyst[a]

propagation	$Zr^{A}_{R_i} + R \xrightarrow{k_{ar}} Zr^{A}_{R_{i+1}}$	(30)
	$Zr^{A}_{R_i} + S \xrightarrow{k_{as}} Zr^{A}_{S_i} + r_i$	(31)
	$Zr^{A}_{S_i} + R \xrightarrow{k_{ar}} Zr^{A}_{R_1} + s_i$	(32)
	$Zr^{A}_{S_i} + S \xrightarrow{k_{as}} Zr^{A}_{S_{i+1}}$	(33)
	$Zr^{B}_{R_i} + R \xrightarrow{k_{br}} Zr^{B}_{R_{i+1}}$	(34)
	$Zr^{B}_{R_i} + S \xrightarrow{k_{bs}} Zr^{B}_{S_1} + r_i$	(35)
	$Zr^{B}_{S_i} + R \xrightarrow{k_{br}} Zr^{B}_{R_1} + s_i$	(36)
	$Zr^{B}_{S_i} + S \xrightarrow{k_{bs}} Zr^{B}_{S_{i+1}}$	(37)
isomerization	$Zr^{A}_{R_i} \underset{k_2}{\overset{k_1}{\rightleftharpoons}} Zr^{B}_{R_i}$	(38)
	$Zr^{A}_{S_i} \underset{k_2}{\overset{k_1}{\rightleftharpoons}} Zr^{B}_{S_i}$	(39)

[a] Zr^{A}_{Ri} is a polymer chain with an isotactic sequence of length i in state A in which each monomer unit possesses the *R* configuration. r_I and s_i are (newly formed) isotactic sequences of length i, where each monomer unit is of *R* and *S* configuration, respectively. *R* and *S*, and k_{ij} are as previously defined (Table 2).

Model Prediction and Simulation of Polymer Crystallinity. From a practical perspective, one is interested in how changes in polymerization conditions (and catalyst structure) influence elastomeric properties in the PP produced using a fluxional catalyst. While the pentad distribution will correlate with these properties, what is needed are predictions about average, isotactic, and atactic block lengths along the chains as well as their distributions and, in particular, the distribution of isotactic block lengths of sufficient length to crystallize.

It is important to recognize that, although the isospecific state will dominate in the formation of isotactic sequences, these sequences will actually be formed by both states (as will the atactic sequences). Thus, the equations depicted in Table 2 for the formation of dyads (*n*-ads etc.) are incomplete to describe all possible origins of isotactic sequences. Rewriting conveniently the kinetic scheme (Table 3),[14] and as outlined in the Supporting Information, it is possible to determine I_A, the average isotactic block length (i.e., independent of the states involved in its formation), and $X(14)$, the weight fraction of isotactic sequences at least 14 monomer units long, the latter value being expected to correlate to the upper limit of total crystallinity of these materials.[15]

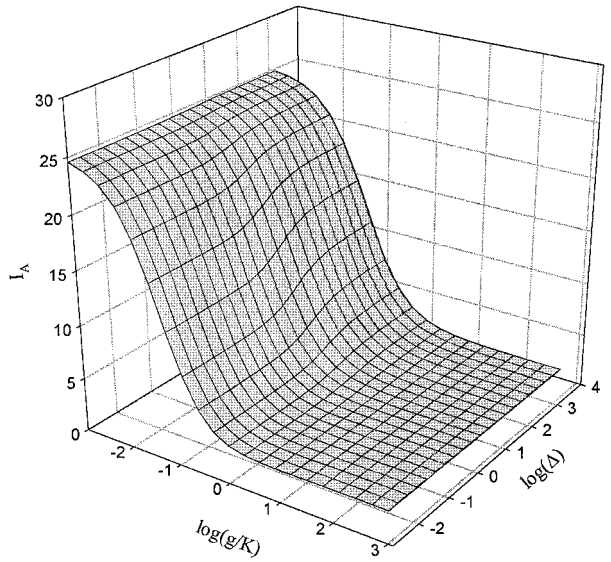

Figure 3. Effect of g/K and Δ upon the average isotactic chain length, I_A ($\alpha = 0.96$, $\beta = 0.5$).

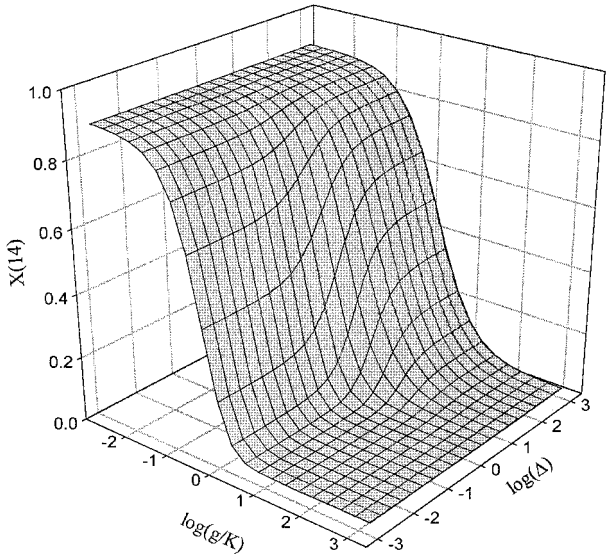

Figure 4. Effect of g/K and Δ on $X(14)$, the mass fraction of isotactic blocks larger than 14 units ($\alpha = 0.96$, $\beta = 0.5$).

The response of these parameters to changes in Δ (i.e., [M]) and g/K are shown in Figures 3 and 4, respectively. As might be expected, these variables change in a similar fashion with Δ and g/K as does the mmmm pentad (Figures 1 and 2), but is interesting to note that their response to changes in Δ and g/K does not exactly parallel that observed for the pentad distribution.

In particular, I_A is much less sensitive to changes in Δ (for a given value of g/K) than the pentad distribution, while $X(14)$ is more sensitive, as one might expect. Also, the values of Δ over which changes in $X(14)$ are evident is somewhat different from that observed for the mmmm pentad.

In essence, the formation of longer isotactic sequences occurs on a longer time scale than formation of pentads, and thus, the corresponding values of Δ (i.e., [M]) required to observe a change in $X(14)$ (i.e., crystallinity) are different. Specifically, at higher values of Δ, while the pentad distribution may be invariant to further changes in [M], $X(14)$ will continue to change with [M], and thus, total crystallinity (and cross-link density) may be affected in this regime.

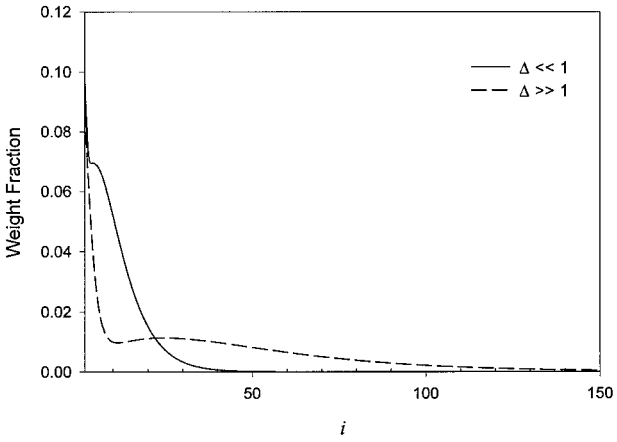

Figure 5. Comparison between the weight isotactic chain length distribution for a polymer produced by a fluxional catalyst in the two limiting regimes: $\Delta \gg 1$ and $\Delta \ll 1$.

The average length of the isotactic and atactic sequences is expected to have a critical influence on the properties of the polymer. One important consequence of a dual-state mechanism for the synthesis of a stereoblock polymer is the prediction that the isotactic and atactic sequences will have a distribution of block lengths, which will depend on the kinetic parameters for enchainment. As shown in Figure 5, the actual isotactic block length distributions, particularly the weight-average, are very different for the limiting values of Δ. For $\Delta \ll 1$, the distribution corresponds to that of a single-state catalyst. For the converse situation, the individual distributions arising from the isospecific and aspecific state overlap but the overall distribution is bimodal.

Monte Carlo algorithms have been successfully used to relate polymer microstructure to polymer crystallinity, particularly in the context of PP.[15] Given the sensitivity of variables related to crystallinity to changes in polymerization conditions, as well as the fundamental kinetic parameters (vide supra), it is interesting to demonstrate these relationships using this technique.

In these simulations, a set of at least 200 polymer chains with $DP_n = 2500$ was generated and aligned in a two-dimensional array that represents a slice of a three-dimensional polymer sample. Each isotactic block was allowed to crystallize if it is longer than 14 units and has a neighboring isotactic block also able to crystallize (also longer than 14 units). Since no chain sliding was performed to simulate the actual chain movement to form crystals, the simulation results lead to a minimum limit to the crystallinity, corresponding to the physical situation in which the polymer melt is quenched.

In Figure 6 are shown the results of these simulations, corresponding to a variety of kinetic situations, which make clear how elastomeric behavior can arise in such systems. In Figure 6, parts A and B, $\Delta < 1$ (i.e., single-state behavior) and the differences between the two figures result from differences in g/K. It can be seen that when $g/K \approx 1$, a homogeneous and essentially amorphous material results. When $g/K \gg 1$ (isospecific state more stable/reactive), the material is also homogeneous but now has appreciable crystallinity which is reminiscent of that observed for i-PP. Conversely, for $\Delta > 1$ (i.e., two-state behavior), Figure 6, parts C and D, shows that a blocky, irregular network structure

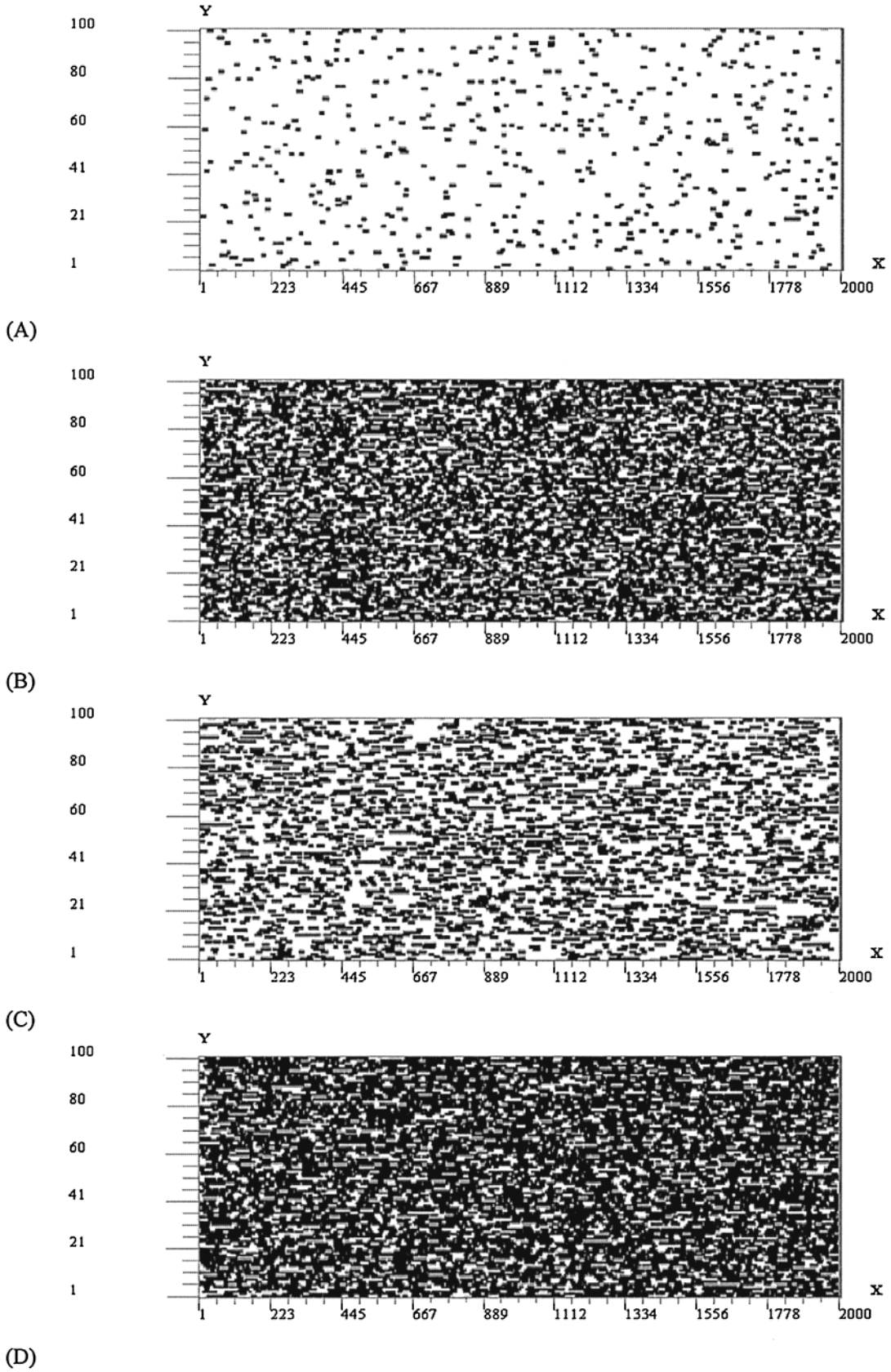

Figure 6. Crystalline regions of a polymer produced by a two-state catalyst with different sets of parameters: (A) $\Delta = 0.1$, $g/K = 1$; (B) $\Delta = 0.1$, $g/K = 20$; (C) $\Delta = 10$, $g/K = 1$; (D) $\Delta = 10$, $g/K = 20$ ($\alpha = 0.96$, $\beta = 0.5$).

results, and the effect of an increase to g/K (Figure 6D) is to decrease the molecular weight between cross-links, as the isopecific state increases in relative reactivity/stability; note the strong similarity between Figure 6D and Figure 6B.

Thus, as suggested earlier, only a limited range of values for the fundamental parameters (g/K, α and β), as well as polymerization conditions, will lead to elastomeric behavior in PP produced with a fluxional catalyst. In particular, if $g/K \gg 1$, the simulation results

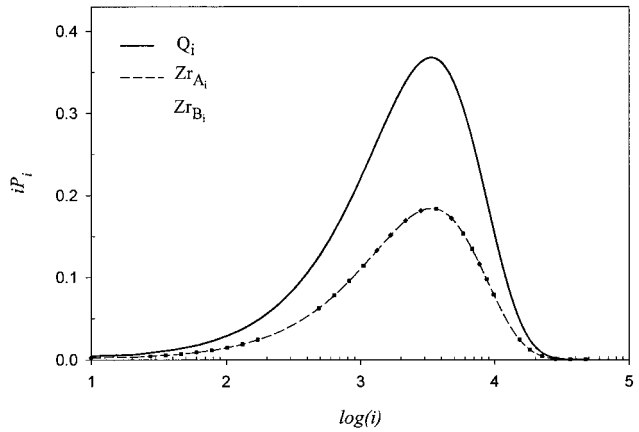

Figure 7. Molecular weight distribution of a polymer produced by a fluxional catalyst with $\Delta = 2.73$ ($K = 1$, $k_{pA}[M] = 1430$ M h^{-1}, $k_{pB}[M] = 4030$ M h^{-1}, $k_{tmA}[M] = k_{tmB}[M] = 0.81$ M h^{-1}, $k_1 = k_2 = 1 \times 10^3$ h^{-1}, DP = 3375, PD = 2.0).

indicate that one may form a tough plastic with properties that approach that of i-PP under all conditions (or amorphous material if $g/K \ll 1$). Ideally, the catalyst must function in a region close to the kinetic quenching limit (for the pentad distribution) in order to control elastomeric properties through changes to experimental conditions (i.e., [M]).

Simulation of the Molecular Weight Distribution. As previously suggested by Coleman and Fox,[11] multistate catalysts can generate polymers with broad molecular weight distributions which may result from slow interconversion of the states during chain growth. As described in the Supporting Information, expressions were obtained that describe the MWD of living and dead polymer chains using mass balance on each species according to the kinetic scheme presented in Table 1.

The MWD of living and dead polymer chains for two, limiting kinetic scenarios are shown in Figures 7 and 8. Here it is assumed that the two states have identical rates of chain transfer (to monomer), are equally stable ($K = 1$) but differ somewhat in their relative propagation rates (i.e., $g = 0.355$).

In Figure 7, the MWD of living and dead chains are depicted for a situation where the isomerization rate is much faster than chain transfer (ca. 1000× faster) but somewhat slower than chain propagation ($\Delta = 2.73$). The living chain distributions are coincident with each other and that of the dead polymer chain distribution all with PD = 2.0. In other words, the two-state catalyst behaves as a single-state catalyst under these conditions as far as the MWD of the polymer produced is concerned.

In Figure 8, the isomerization rate is much slower than chain transfer (by about a factor of 10^4!) giving rise to a dead polymer chain length distribution with PD = 2.5 and living chain distributions which are no longer coincident. It is obvious that the MWD of dead polymer chains is only significantly broadened when the rate of isomerization is much slower than that of chain transfer, particularly if the states do not differ significantly in their k_p/k_{tr} characteristics, as in this example. This is easily understood, as in this regime, the two states function essentially independently from each other and a (possibly compatibilized) blend of two polymers is obtained.

In Figure 9, the PD of the dead polymer, produced by a fluxional catalyst with $g = K = 1$ and $k_{pA}/k_{tmA} = 10^4$,

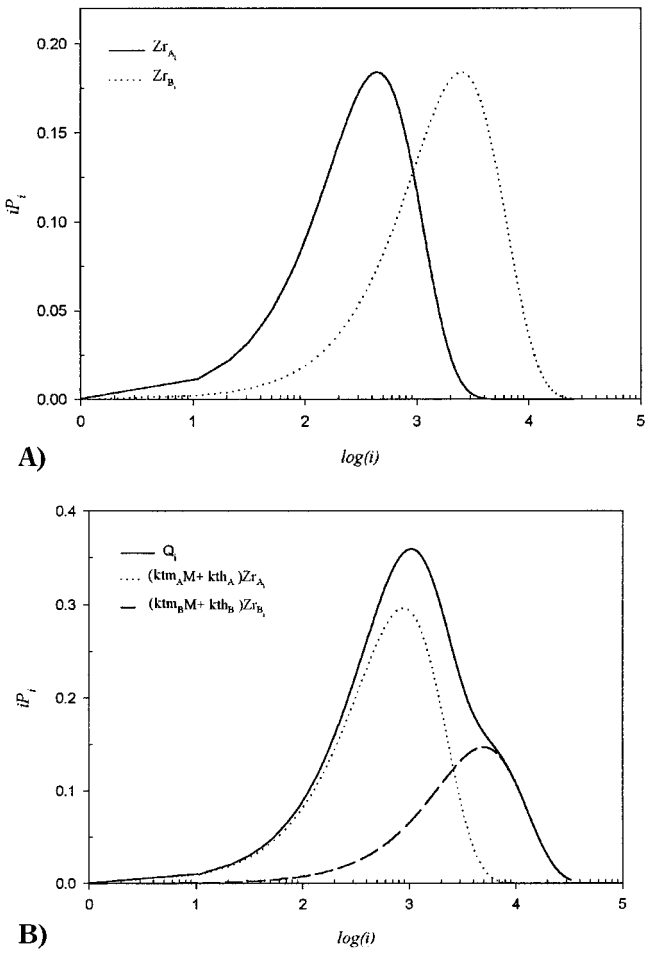

Figure 8. (A) Molecular weight distribution of the living polymer produced by a fluxional catalyst with $\Delta = 2.73 \times 10^7$. (B) Molecular weight distribution of the dead polymer produced by a fluxional catalyst with $\Delta = 2.73 \times 10^7$ ($K = 1$, $k_{pA}[M] = 1430$ M h^{-1}, $k_{pB}[M] = 4030$ M h^{-1}, $k_{tmA}[M] = 0.81$ M h^{-1}, $k_{tmB}[M] = 0.81$ M h^{-1}, $k_1 = k_2 = 1 \times 10^{-4}$ h^{-1}, DP = 2243, PD = 2.5).

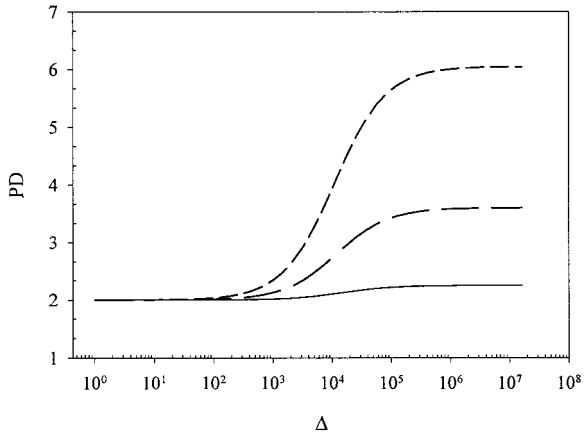

Figure 9. Effect of increasing Δ upon the polydispersity ($g = K = 1$, $k_{pA} = k_{pB} = 1$ h^{-1}, $k_{thB} = k_{thA} = 0$, $k_{tmA} = 1 \times 10^{-4}$ h^{-1}; — $k_{tmB}/k_{tmA} = 2$ (DP = 6700), - - - $k_{tmB}/k_{tmA} = 5$ (DP = 3335), ··· $k_{tmB}/k_{tmA} = 10$ (DP = 1820)).

is plotted against Δ (i.e., [M]) for various ratios of the chain transfer constants for the two states, and it is obvious from this graph that in order to observe detectable broadening of the MWD beyond the Schultz−Flory value (i.e., PD = 2), that $\Delta > 10^{-1}$(DP) if the two states differ in their k_p/k_{tr} characteristics. Moreover, as is also evident from this figure, detectable broadening of the

Table 4. Propylene Polymerization Using 2-Arylindenyl Metallocene Complexes 1 and 2[a]

expt	catalyst	$[C_3H_6]$ (M)	mmmm[b]	$10^{-3}M_n$[c]	PD[c]
1	1	1.2	0.15	29.0	2.0
2	1	1.2	0.15	30.0	2.0
3	1	2.2	0.19	43.3	2.0
4	1	2.2	0.21	43.1	2.1
5	1	2.8	0.22	55.4	2.1
6	1	2.8	0.23	59.6	2.1
7	1	3.8	0.24	66.7	2.1
8	1	3.8	0.25	72.5	2.3
9	1	bulk	0.30	96.6	2.4
10	2	1.8	0.21	48.0	2.8
11	2	3.1	0.26	59.0	3.2
12	2	5.0	0.30	108.0	4.1
13	2	5.0	0.33	88.0	5.3
14	2	bulk	0.30	97.1	4.7

[a] For conditions see Experimental Section. [b] Measured from the ^{13}C NMR spectrum and normalized to unity. [c] Determined by GPC.

MWD is observed at somewhat lower values of Δ, as the difference in the k_p/k_{tr} characteristics of each state increases.

These findings should be contrasted to the conclusions made earlier about the pentad distribution, where changes are observed in the absolute range $10^{-1} < \Delta < 10^2$. Thus, for any polymerization leading to the formation of polymer (i.e., DP ≥ 10^3), the MWD should be close to the Schultz-Flory value if the pentad distribution is changing in response to changes in monomer concentration. Conversely, if the MWD does respond to changes in [M], by definition the pentad distribution should not. Thus, it is difficult to reconcile previously observed behavior of 2-arylindene metallocene catalysts[1,3] using this model unless there are other factors responsible for broadening the MWD (vide infra).

Application of the Model to Unbridged 2-Arylindene Catalyst Systems: Pentad Distributions. We chose to apply this model to two, prototypical fluxional catalyst systems, namely (2-PhInd)$_2$ZrCl$_2$ (in combination with MAO; **1**)[3] and the *p*-CF$_3$Ph analogue **2**.[16] The behavior of the former system has been studied in some detail, most recently with reference to the polymerization behavior of two *ansa*-metallocenes, *rac*- and *meso*-Me$_2$Si(2-PhInd)$_2$ZrCl$_2$ (**3** and **4**, respectively), which may serve as models for the individual states involved in polymerizations using **1**.[3c]

Complexes **1** and **2** afford PP with similar microstructures, although the pentad distributions respond somewhat differently to changes in monomer concentration, suggesting that the relative stability/reactivity of the two states (g/K), the intrinsic stereoselectivities (α and β), and/or the catalyst operating regime (Δ) have been subtly influenced.

Previous polymerizations involving the use of catalysts **1** and **2** provided PP with a broad, but largely unimodal MWD.[17] Given the theoretical discussion above, it is not obvious how these two effects can be reconciled using this two-state model, without additional hypotheses, as the values of Δ required to observe broadening of the MWD are quite different from those where changes in the pentad distribution are expected.

More recent work using complex **1**, in which the monomer concentration was constant (and well-known) during polymerization has revealed that the MWD observed are considerably narrower (PD = 2.0−2.4 in going from [M] = 1−10 M) although the pentad distribution still changes with [M] (Table 4).[18] Furthermore,

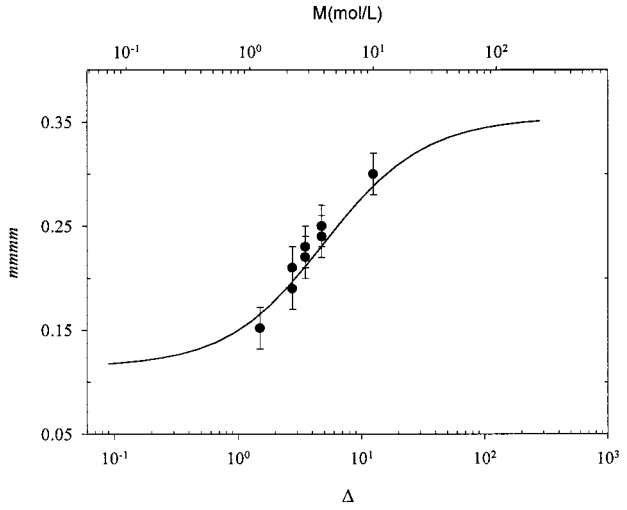

Figure 10. Theoretical curve of % mmmm vs Δ and [M] for catalyst **1** with experimental points shown.

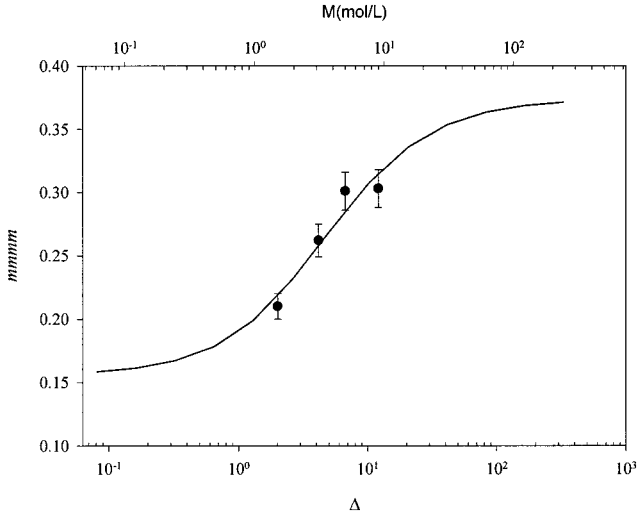

Figure 11. Theoretical curve of % mmmm vs Δ and [M] for catalyst **2** with experimental points shown..

as will be reported in detail elsewhere,[18] the principal chain transfer process observed using complex **1** is β-H elimination, and thus, DP at any time will be directly proportional to [M]. If [M] is not constant during polymerization, this could account for the breadth of the MWD seen in earlier work involving complex **1**.[19]

The responses of the mmmm pentad (in %) for PP produced using **1** and **2** to changes in [M] are depicted in Figures 10 and 11, respectively, along with theoretical curves that were generated using the kinetic model. The values of g/K, α, β, and k_{p_B}/k_2 (i.e., indirectly Δ/[M]—see eq 3) were allowed to vary so as to minimize the residual sum of squares between all nine experimental pentads and the theoretical ones at each monomer concentration. Note that we have included two *x* axes in these figures, one in terms of Δ and the other in terms of [M], which will be offset with respect to each other, depending on the magnitude of the constant = $^1/_2[(g/K) + 1][k_{p_B}/k_2]$.

Initially, it was assumed that enantiomorphic site control was operative for both states using catalyst **1**, but this resulted in values of $\beta < 0.5$ for the aspecific state—clearly a nonsensical result (fit not shown). Instead, a modified version of the model, which incorporates chain-end control for the aspecific state was used and provided more satisfactory results in the case

Table 5. Best Fit Parameters for 2-Arylindenyl Metallocene Complexes 1 and 2 and Representative Pentad Distributions[a]

expt[b]	mmmm	mmmr	rmmr	mmrr	xmrx	mrmr	rrrr	mrrr	mrrm
4	0.21	0.15	0.05	0.14	0.18	0.10	0.03	0.07	0.06
calcd	0.20	0.15	0.04	0.13	0.18	0.09	0.05	0.10	0.06

		parameters[c]			
complex	Δ/[M][d]	g/K	α	β	RSS ($\times 10^3$)
1	1.3	0.60	0.97	0.44[e]	1.7

expt[b]	mmmm	mmmr	rmmr	mmrr	xmrx	mrmr	rrrr	mrrr	mrrm
10	0.21	0.15	0.05	0.13	0.19	0.10	0.04	0.08	0.06
calcd	0.22	0.16	0.04	0.12	0.20	0.09	0.03	0.08	0.06

		parameters[c]			
complex	Δ/[M][d]	g/K	α	β	RSS ($\times 10^3$)
2	2.5	0.69	0.97	0.50	0.70

[a] For the fit of the model to the experiments summarized in Table 4, see Figures 10 and 11. [b] The experiment number refers to entries in Table 4. [c] The parameters listed are those which result from the best fit of the model to all of the experimental data. [d] $\Delta/[M] = {}^1/_2[g/K + 1](k_{p_B}/k_2)$; the quantity (k_{p_B}/k_2) was the independent parameter used in the modeling. [e] $\beta = P_m$ the probability of meso dyad formation by a chain-end control mechanism − see text.

of complex **1** (Figure 10). The best-fit parameters are listed in Table 5 along with representative experimental and theoretical pentad distributions; note that β in Table 5 for catalyst **1** is now defined as the probability of forming a *meso* dyad ($P_m = 1 - P_r$). It is interesting to note that the best fit suggests a slight tendency for the aspecific state to produce s-PP by a chain end control mechanism [$P_r = 0.56$].

In the case of complex **2**, a satisfactory fit of the model to the data could be obtained by assuming that the aspecific state produced perfectly atactic PP via a site-control mechanism (i.e., $\beta = 0.5$, Figure 11, Table 5).

The best-fit values of these parameters are presented in Table 5. All estimated parameters for catalysts **1** and **2** showed a moderate, negative, linear correlation (the maximum correlation coefficient for these parameters was −0.7) indicating that the model is reasonably well behaved. The fit of calculated intensities to experimental data is excellent for both (RSS $\approx 1 \times 10^{-3}$, i.e., ±3%). It is interesting to notice that the estimated parameters for **1** are similar to those estimated using rate and stereoselectivity data from the *ansa*-metallocene analogues **3** and **4**.[3c]

It is appropriate to discuss error limits to the parameters obtained from modeling. Since Δ can only be varied over a narrow range experimentally (i.e., basically an order of magnitude—see Figures 10 and 11), it is not clear exactly where one is on the "linear" portion of the curve connecting the two limiting regimes (C−H and KQ). That is, to determine an accurate range for Δ, significant curvature should ideally be observed in a plot of mmmm vs Δ (note that the scales for both Δ and [M] are logarithmic).

The pentad distributions produced using catalysts **1** and, to a lesser extent, **2** do not show asymptotic behavior over the range of [M] studied so that the uncertainty in Δ has some effect on the values of the fundamental parameters that ensue from modeling of the pentad distributions.

Shown in Table 6 are the fits of the model to the data (RSS) for catalyst **2**, as well as the values of the parameters estimated from the model, where the value of Δ/[M] was varied from 0.1 to about 100. In particular, given the uncertainty in Δ, as well as that associated with measurement of the pentad distribution, α could vary from about 0.93 to 1.0 with g/K between 0.72 and 0.60 for $\beta = 0.5$. Note that one can automatically exclude the possibility that complex **2** operates under C−H conditions, because nonsensical estimates of α are predicted (entries 1 and 2, Table 6) while conditions that approach KQ seem to be also inappropriate as the mmmm pentad exhibits saturation behavior (entries 6 and 7).

Table 6. Variation in Model Parameters as a Function of Δ/[M] for Catalyst 2[a]

entry	Δ/[M]	α	g/K	RSS
1	0.1	1.71	0.25	0.0037
2	0.9	1.02	0.71	0.0020
3	1.7	0.98	0.72	0.0016
4	8.1	0.94	0.62	0.0021
5	16.0	0.93	0.60	0.0027
6	40.8	0.92	0.63	0.0034[b]
7	82.0	0.91	0.64	0.0036[b]

[a] $\Delta/[M] = {}^1/_2[g/K + 1](k_{p_B}/k_2)$ and is thus independent of experimental conditions. [b] The mmmm pentad is already approximately constant at mmmm = 0.28.

While dyad analysis may provide a more accurate range for Δ, as dyads are formed on a shorter time scale than pentads (i.e., 2.5× shorter), modeling of the dyad distribution for **1** as a function of Δ revealed that saturation behavior was also not observed.[20]

In Figure 12 is depicted the calculated, (weight-average) isotactic stereoblock distribution and some average quantities for that distribution, for the polymer produced by **1** in liquid propylene, and for the sake of comparison, a distribution obtained with the same model parameters, but $\Delta \ll 1$. It should be clear from Figure 12 and the calculated breadth of the distribution (PD = 2.4), that there is a significant broadening of the isotactic stereoblock distribution, in relation to the one obtained with a single-site catalyst (PD = 1.4), due to the comparatively slow isomerization process. As should be expected, this broadening is much smaller than the one that would be obtained if $\Delta \gg 1$ (not shown in the figure—in this case PD ∼ 6).

Statistical models for the description of polymer structure frequently include, either deliberately, or as a result of the model assumptions, a block length (BL) and it is appropriate to relate this to the calculated, block length distributions obtained using a kinetic

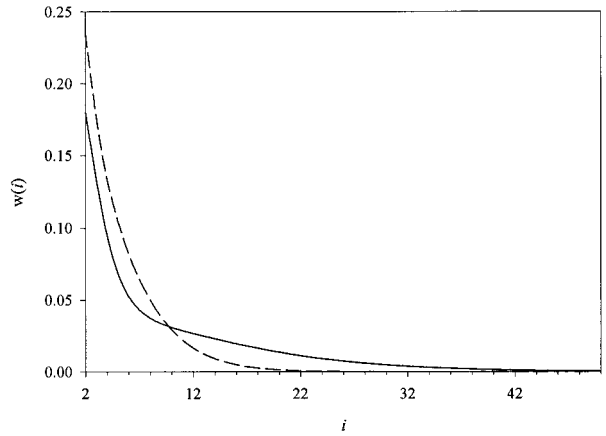

Figure 12. (—) Calculated weight isotactic stereoblock distribution for polypropylene produced by **1** in liquid propylene [$I_A = 4.4$, PD = 2.4, $X(14) = 0.22$, I_{NC} (number-average length of a crystallizable sequence) = 23, I_{WC} (weight-average length of a crystallizable sequence) = 26]. (- -) Calculated weight isotactic stereoblock distribution for polypropylene hypothetically produced by **1** if $\Delta \ll 1$ ($I_A = 3.6$, PD = 1.4).

model (e.g., Figures 5 and 12). Chujo's two-state model[21] would approximate the behavior of a 2-arylindene metallocene catalyst under KQ conditions, and would give an exact answer when the two states operate independently [i.e. $BL_i = DP_i$ (i = A, B)]. Models based on the hypothesis of $BL_i \geq 5$ monomer units[5,22] are obviously valid over a broader range of conditions. However, they exclude a significant portion of the surface where the polymer is predicted to be semicrystalline (Figure 4) and where elastomeric properties may arise.

It is important to notice the reasonable agreement between properties estimated from the model and the experimental data. The maximum crystallinity [$X(14)$] was estimated to be 0.22, very close to, but obviously higher than, the experimental values obtained from heat of fusion and X-ray diffraction measurements (0.11 and 0.15, respectively).[2c]

The model can also be used to estimate the number and weight-average lengths of a crystallizable sequence ($I_{NC} = 23$, $I_{WC} = 26$, respectively). The former value is expected to be a *lower* limit for the actual, average length of the crystalline units, but it is gratifying that it is of the same magnitude as that estimated by atomic force microscopy ($I_{NC} = 54$).[23]

The calculated, number and weight-average length of the amorphous sequences between crystalline domains are $I_{NA} = 90$ and $I_{WA} = 175$, respectively. These values should correspond to an *upper* limit for the molecular weight between cross-links ($M_{n,a}$), which can be estimated from measurement of the equilibrium storage modulus.

Recent work has shown that for samples of elPP produced using **1** in liquid propylene, $M_{n,a} = 900$ or $I_{NA} \sim 21$.[2b] This analysis used simple elasticity theory to evaluate the results and did not take into account the physical dimensions of the tie-points (or their variable crystallinity), as well as the probability of chain entanglements in the amorphous regions;[24] the experimental value is therefore a *lower* limit to $M_{n,a}$ and it is gratifying that the experimental and theoretical results are in the expected order.

This agreement between calculated and observed physical properties (within the limitations of both the model and experiments) suggests that the model developed will prove useful in predicting physical properties from the observed pentad distribution or conversely, by using the measured physical properties to establish upper or lower confidence limits for model parameters estimated from the pentad distribution.

Table 7. Model Parameters Estimated from MWD of PP Produced Using Complex 2[a]

experiment[b]	10	11	14
$(k_{tm_A}[M] + k_{th_A})/k_{p_A} \times 10^3$	2.53	3.51	7.75
$(k_{tm_B}[M] + k_{th_B})/k_{p_B} \times 10^3$	1.16	1.44	1.37
τ_1 (min)	3.7	2.8	2.2
g/K		0.48	
$k_1/k_{p_A} \times 10^4$		0.64	
$k_2/k_{p_B} \times 10^4$		0.31	
τ_2 (min)		~30	

[a] For definition of symbols see text and also Table 1. [b] The experiment no. corresponds to the entries shown in Table 4.

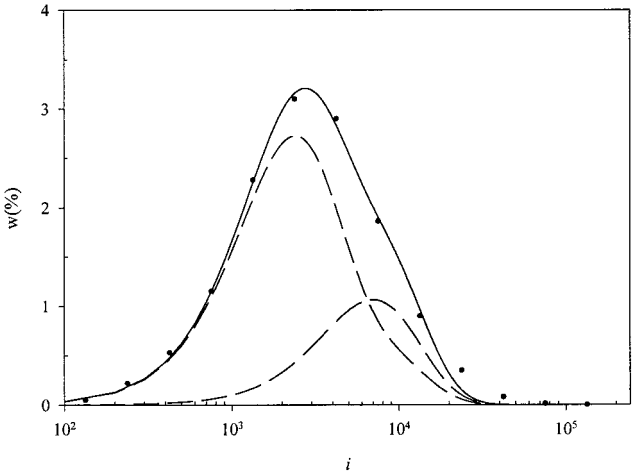

Figure 13. MWD deconvolution for the PP produced by catalyst **2** at 20 °C and $[C_3H_6] = 3.1$ M (···, calculated molecular weight distribution of the polymer produced by each state; - - -, calculated total polymer molecular weight distribution; ●, experimental polymer molecular weight distribution).

Application of the Model to 2-Arylindenyl Catalyst Systems: Molecular Weight Distributions. Even though the MWD of polymers prepared using complex **2** are broad, but largely unimodal in nature, it is instructive to de-convolute the MWD to demonstrate that significantly different estimates of the model parameters result compared to those estimated from the pentad distribution.

The usual procedure of fitting one GPC at each time, although easier and less computationally demanding, proved to be inadequate as slightly different values of g/K were estimated from each MWD at each monomer concentration. Therefore, the de-convolution was carried out using all the available GPC data at the same time. The estimated parameters are shown in Table 7, and a typical de-convoluted MWD is depicted in Figure 13.

If we assume that chain transfer reactions have no effect on the state-to-state interconversion, we can define an average time between isomerizations by

$$\tau_2 = \left(\frac{R_p + (k_1\Psi + k_2(1-\Psi))}{(k_1\Psi + k_2(1-\Psi))R_p} \right) \tag{5}$$

while the average chain lifetime is given by

$$\tau_1 = \frac{DP}{R_p} \tag{6}$$

On the basis of the activity data, and assuming for sake of simplicity that all the metallocene present in the reactor is active, for catalyst **2**, τ_1 and τ_2 would have to be approximately 3 and 30 min, respectively (Table 7) based on the breadth of the observed MWD. It is important to mention that τ_2 is connected to τ_1 through the calculation of the average time for one monomer insertion, so it would be more appropriate to say that τ_2 would have to be about 5−10 times longer than the chain lifetime.

Thus, modeling of the MWD of PP produced using catalyst **2** demonstrates that isomerization would have to be much slower that the rate of polymerization. This is completely inconsistent with the conclusions which ensued from the analysis of pentad data (vide supra). Given the more recent results using **1** that show the MWD is considerably narrower at constant monomer concentration, we suspect that the broad MWD observed in PP prepared using **2** also results, in part, from this feature (i.e., variation in [M] during polymerization).

Conclusions

A kinetic model that can be used to describe the propylene polymerization behavior of a two-state, fluxional catalyst, over a wide range of experimental conditions, was developed and employed in the case of two prototypical examples of 2-arylindenylmetallocene catalysts. The modeling of MWD and pentad distributions led to antagonistic results—the breadth of MWD suggests that the catalyst isomerization takes place very slowly, compared to monomer insertion, while the pentad distribution results suggest that the catalyst isomerization takes place at comparable rates to this process. Part (or possibly all) of the broadening seen in the MWD in earlier work may be related to variable monomer concentrations during polymerization.

Experimental Section

General Comments. Number and weight-average molecular weights (M_n and M_w) were obtained using a Waters 150C high-temperature chromatograph. Samples were run in 1,2,4-trichlorobenzene at 139 °C using two Polymer Laboratories PL GEL mixed-bed columns at a flow rate of 1 mL/min. Polymer microstructure was determined from the methyl pentad region of the polymer ^{13}C NMR spectrum. ^{13}C NMR spectra were recorded on a Varian Inova-300 spectrometer operating at 75 MHz and 100 °C with a 45° pulse width and no relaxation delay between pulses. Samples were prepared by dissolving the polymer in a mixture of TCE/TCE-d_2 at 100 °C. All pentad and MWD simulations/modeling were performed on an PC computer, using locally written routines in Fortran. Currently the modeling software is not very convenient to use because individual lines in the Fortran code must be modified for different conditions/model parameters. A more accessible user interface is planned in the future. and copies will be made available on request when this occurs.

Procedure for Propylene Polymerization. All catalyst and MAO solutions were prepared in a Vacuum Atmospheres drybox which had been purged for 5 min; $[O_2] \sim 0-2$ ppm. Catalyst and MAO were weighed using a Mettler Toledo AB204 balance. Toluene used in preparing catalyst and MAO solutions was purchased from Aldrich and purified over alumina/copper oxide. Polymerizations were carried out in a 300 mL stainless steel Parr reactor. The Parr reactor bottom and stirrer was baked out in a glassware oven, and the assembled reactor was then pumped down to < 60 mTorr on a vacuum line, refilled with dry N_2, and purged with propylene. An MAO/toluene solution (98 mL) was placed in the Parr reactor under propylene pressure and was equilibrated at the polymerization pressure for 60−75 min. A solution of (2-PhInd)$_2$ZrCl$_2$ in toluene (2 mL) was then introduced to the reactor under propylene pressure. The polymerization was quenched using 10 mL methanol delivered under Ar pressure. The reactor was vented down to atmospheric pressure and the resulting toluene/methanol solution was added to 500 mL acidic methanol to precipitate the polymer. After stirring overnight, the polymer was recovered via filtration and dried in a 40 °C vacuum oven for several hours.

Acknowledgment. M.N., M.L.D., and J.C.P. wish to thank CNPq (Conselho Nacional de Pesquisa e Desenvolvimento), Brazil, and Polibrasil Resinas S.A. for providing a scholarship and for financial support of this research. S.C. and M.N. wish to thank the Natural Sciences and Engineering Research Council of Canada for financial support. S.L. and R.M.W. thank the NSF for financial support of this work.

Supporting Information Available: Model description and derivation of expressions governing MW and MW distributions, dyad and pentad distributions, average block lengths produced by each state (BL_i, i = A,B), average isotactic sequence lengths (I_A) and weight fraction of crystallizable sequences [X(14)] for fluxional metallocene catalysts. This material is available free of charge via the Internet at http://pubs.acs.org.

References and Notes

(1) (a) Kaminsky, W.; Buschermohle, M. in *Recent Advances is Mechanistic and Synthetic Aspects of Polymerization*; Fontanille, M., Guyot, A., Ed.; Reidel: New York, 1987; pp 503−514. (b) Erker, G.; Nolte, R.; Tsay, Y. H.; Krueger, C. *Angew. Chem.* **1989**, *101*, 642. (c) Erker, G.; Aulbach, M.; Knickmeier, M.; Wingbermuhle, D.; Kruger, C.; Nolte, M.; Werner, S. *J. Am. Chem. Soc.* **1993**, *115*, 4590. (d) Razavi, A.; Atwood, J. L. *J. Am. Chem. Soc.* **1993**, *115*, 7529. (e) Rieger, B.; Jany, G.; Fawzi, R.; Steimann *Organometallics* **1994**, *13*, 647. (f) Coates, G. W.; Waymouth, R. M. *Science* **1995**, *267*, 217. (g) Knuppel, S.; Faure, J. L.; Erker, G.; Kehr, G.; Nissinen, M.; Frohlich, R. *Organometallics* **2000**, *19*, 1262.

(2) (a) Collete, J. W.; Ovenall, D. W.; Buck, W. H.; Ferguson, R. C. *Macromolecules* **1989**, *22*, 3858. (b) Carlson, E. D.; Krejchi, M. T.; Shah, C. D.; Terakawa, T.; Waymouth, R. M.; Fuller, G. G. *Macromolecules* **1998**, *31*, 5343. (c) Hu, Y.; Krejchi, M. T.; Shah, C. D.; Myers, C. L.; Waymouth, R. M. *Macromolecules* **1998**, *31*, 6908.

(3) (a) Hauptman, E.; Waymouth, R. M.; Ziller, J. W. *J. Am. Chem. Soc.* **1995**, *117*, 11586. (b) Kravchenko, K.; Masood, A.; Meyers, C. L.; Waymouth, R. A. *J. Am. Chem. Soc.* **1998**, *120*, 2039. (c) Petoff, J. L. M.; Agoston, T.; Lal, T. K.; Waymouth, R. M. *J. Am. Chem. Soc.* **1998**, *120*, 11316.

(4) Coleman, B. D.; Fox, T. G. *J. Chem. Phys.* **1963**, *38*, 1065.

(5) Cheng, H. N.; Babu, G. N.; Newmark, R. A.; Chien, J. C. W. *Macromolecules* **1992**, *25*, 6980.

(6) Bruce, M. D.; Waymouth, R. M. *Macromolecules* **1998**, *31*, 2707.

(7) The use of a kinetic model to describe PP stereo-sequence length distributions using noninterconverting, multisite, Ziegler−Natta catalysts has been reported. De Carvalho, A. B. M.; Gloor, P. E.; Hamielec, A. E. *Polymer* **1990**, *31*, 1290.

(8) Shaffer, W. K. A.; Ray, W. H. *J. Appl. Polym. Sci.* **1997**, *65*, 1053; see pp 1072−1074.

(9) First-order kinetics are assumed—other kinetic orders in [M] can be treated but additional states may need to be invoked. For a review of kinetics of propylene polymerization using metallocene catalysts, see: Resconi, L.; Cavallo, L.; Fait, A.; Piemontesi, F. *Chem. Rev.* **2000**, *100*, 1253−1346.

(10) (a) Shelden, R. A.; Fueno, T.; Tsunetsugu, T.; Furukawa, J. *J. Polym. Sci., Polym. Lett. Ed.* **1965**, *3*, 23. (b) Bovey, F. A.; Tiers, G. V. D. *J. Polym. Sci.* **1960**, *44*, 173.

(11) This aspect was first discussed in the context of living polymerization—see: Coleman, B. D.; Fox, T. G. *J. Am. Chem. Soc.* **1963**, *85*, 1241.

(12) Press, W. H.; Teukollky, S. A.; Vetterline, W. T.; Flanney, B. P. In *Numerical Recipes in Fortran 77*, 2nd ed.; Cambridge University Press: Cambridge, U.K., 1992.

(13) (a) Bravaskis, A. M.; Bailey, M. P.; Pigeon, M.; Collins, S. *Macromolecules* **1998**, *31*, 1000. (b) Mohammed, M.; Xin, S.; Collins, S. *Am. Chem. Soc. PMSE Prepr.* **1999**, *80*, 441. (c) Nele, M. N.; Mohammed, M.; Xin, S.; Pinto, J. C.; Collins, S. Manuscript in preparation.

(14) Zaldivar, C.; Iglesias, G.; del Sol, O.; Pinto, J. C. *Polymer* **1997**, *38*, 5823.

(15) Tarek, M. M.; Mark, J. E. *J. Appl. Polym. Sci., Part B: Polym. Phys.* **1997**, *35*, 2757.

(16) Lin, S.; Hauptman, E.; Lal, T.; Waymouth, R. M.; Quan, R. W.; Ernst, A. B. *J. Mol. Catal. A: Chem.* **1998**, *136*, 23.

(17) Other related systems actually produce PP with a bimodal MWD but their response to changes in $[C_3H_6]$ etc. have not been investigated in sufficient detail: Witte, P.; Lal, T. K.; Waymouth, R. M. *Organometallics* **1999**, *18*, 4147.

(18) Lin, S.; Tagge, C. T.; Waymouth, R. M.; Nele, M. N.; Pinto, J. C.; Collins, S. *J. Am. Chem. Soc.*, submitted for publication.

(19) The two factors that led to variations in [M] during polymerization (and thus DP) are high rates of polymerization coupled with decreasing rates of monomer diffusion with increasing, dissolved polymer concentrations.[18] It is important to emphasize that any catalyst which is very active and produces high MW, low-tacticity PP (i.e. soluble in the reaction medium) could produce PP with a broad MWD under similar conditions.

(20) Nele, M. N. Unpublished results.

(21) Inoue, Y.; Itabashi, Y.; Chûjo, R.; Doi, Y. *Polymer* **1984**, *25*, 1640.

(22) (a) Cheng, H. N.; Babu, G. N.; Newmark, R. A.; Chien, J. C. W. *Macromolecules* **1992**, *25*, 7400. (b) Gauthier, W. J.; Collins, S. *Macromolecules* **1995**, *28*, 3779.

(23) Kravchenko, R. L.; Sauer, B. B.; McLean, R. S.; Keating, M. Y.; Cotts, P. M.; Kim, Y. H. *Macromolecules* **2000**, *33*, 11.

(24) Carlson, Eric D. Private communication.

MA000401Z